

Report Number 10/36

**Sequential Inverse Problems Bayesian Principles and the Logistic
Map Example**

by

Lian Duan, Chris L. Farmer, and Irene M. Moroz



Oxford Centre for Collaborative Applied Mathematics
Mathematical Institute
24 - 29 St Giles'
Oxford
OX1 3LB
England

Sequential Inverse Problems Bayesian Principles and the Logistic Map Example

Lian Duan*, Chris L. Farmer* and Irene M. Moroz†

*Oxford Centre for Collaborative Applied Mathematics, Mathematical Institute, University of Oxford, OX1 3LB

†Oxford Centre for Industrial and Applied Mathematics, Mathematical Institute, University of Oxford, OX1 3LB

Abstract. Bayesian statistics provides a general framework for solving inverse problems, but is not without interpretation and implementation problems. This paper discusses difficulties arising from the fact that forward models are always in error to some extent. Using a simple example based on the one-dimensional logistic map, we argue that, when implementation problems are minimal, the Bayesian framework is quite adequate. In this paper the Bayesian Filter is shown to be able to recover excellent state estimates in the *perfect model scenario* (PMS) and to distinguish the PMS from the *imperfect model scenario* (IMS). Through a quantitative comparison of the way in which the observations are assimilated in both the PMS and the IMS scenarios, we suggest that one can, sometimes, measure the degree of imperfection.

Keywords: Logistic Map, Bayesian Filter, Grid Based Method, Hellinger Distance, Distinguishing the Prefect and Imprefect Scenarios

PACS: 02.50.Ng, 05.45.Tp, 02.50.Cw, 02.50.Le, 05.45.Ac

INTRODUCTION

In many problems such as that of weather or hydrocarbon reservoir forecasting one must characterise the initial state of knowledge using a probability density function (pdf). The non-linearity of the models makes it difficult to evolve this initial pdf and makes it difficult to assimilate any new measurements. The logistic map: $x_{t+1} = 1 - ax_t^2$, with $x_t \in [-1, 1]$, $a \in [0, 2]$ provides a very simple example of this situation. The *inverse* problem requires an estimation of x_t and a , given a sequence of noisy observations, $s_t = x_t + v_t$, where v_t is the noise. Methods for solving inverse problems associated with such chaotic or unstable systems starts with Berliner [1], who introduces the inverse problem for the logistic map and proposes a Bayesian solution. The *maximum a posteriori* method is used and gives good results when the data are observed from the true system, a situation termed the *perfect model scenario* (PMS) by Judd and Smith [2]. The more realistic case, of course, is when observations are taken from an unknown physical system, which differs from the model. We are then in the *imperfect model scenario* (IMS) of Judd and Smith [3].

In this paper, we derive the exact analytical solution of the Bayesian filter for the logistic map. Using numerical experiments in the PMS, the performance of the Bayesian filter is examined with a grid-based method. Finally, we use the Hellinger distance [6] between the prior and posterior pdfs, to distinguish between the PMS and IMS scenarios.

EXACT SOLUTION OF BAYESIAN FILTER

Assume the logistic map, $x_{t+1} = 1 - ax_t^2$, with $t \in \{0, 1, 2, \dots\}$, $x_t \in [-1, 1]$ and $a \in [0, 2]$ has been chosen to model a time series of noisy observations s_t , given by $s_t = x_t + v_t$, where the noise v_t is sampled independently from a Gaussian distribution, π_σ , with zero mean and known variance σ^2 . The vector of observations $\{s_m\}_{m=1}^M$ is denoted by S_M . Note the choice not to observe the initial state. Finally, we assume that a prior joint pdf, $\pi_0(x_0, a)$, for x_0 and a has been provided. We will focus on the following two problems:

The prediction problem

Suppose that a pdf $\pi(x_t, a|S_t)$ has been found at time t . Using independence of the variables and properties of the delta function, the prior pdf, $\pi(x_{t+1}, a|S_t)$, at time $t + 1$ is given by

$$\pi(x_{t+1}, a|S_t) = \int_{-1}^1 \pi(x_{t+1}, x_t, a|S_t) dx_t = \int_{-1}^1 \pi(x_{t+1}|x_t, a) \pi(x_t, a|S_t) dx_t. \quad (1)$$

Substituting for x_t from the logistic map into equation (1) and evaluating the integral using properties of the delta function, we obtain

$$\tilde{\pi}_{t+1}(x_{t+1}, a | S_t) = \frac{1}{\sqrt{4a(1-x_{t+1})}} \left\{ \pi_t\left(\sqrt{\frac{1-x_{t+1}}{a}}, a | S_t\right) + \pi_t\left(-\sqrt{\frac{1-x_{t+1}}{a}}, a | S_t\right) \right\}, \quad (2)$$

where $\tilde{\pi}_{t+1} = 0$ for $x_{t+1} < (1-a)$ and $t > 0$.

The filtering problem

Suppose that a measurement s_{t+1} is received at time $t+1$. Standard methods from probability theory give

$$\pi_{t+1}(x_{t+1}, a, s_{t+1} | S_t) = \pi_{t+1}(s_{t+1} | x_{t+1}, a, S_t) \tilde{\pi}_{t+1}(x_{t+1}, a | S_t) = \pi_{t+1}(s_{t+1} | x_{t+1}, a) \tilde{\pi}_{t+1}(x_{t+1}, a | S_t). \quad (3)$$

Substituting for the observation model and equation (2) into equation (3), we obtain

$$\pi_{t+1}(x_{t+1}, a, s_{t+1} | S_t) = \frac{\pi_\sigma(x_{t+1} - s_{t+1})}{\sqrt{4a(1-x_{t+1})}} \left\{ \pi_t\left(\sqrt{\frac{1-x_{t+1}}{a}}, a | S_t\right) + \pi_t\left(-\sqrt{\frac{1-x_{t+1}}{a}}, a | S_t\right) \right\}, \quad (4)$$

where $\pi_{t+1} = 0$ for $x_{t+1} < (1-a)$ and $t > 0$. Equation (4) is similar in form to that for the Perron-Frobenius map [4]. Finally, applying Bayes' rule, one deduces that

$$\pi_{t+1}(x_{t+1}, a | S_{t+1}) = \frac{\pi_\sigma(x_{t+1} - s_{t+1}) \tilde{\pi}_{t+1}(x_{t+1}, a | S_t)}{\int_0^2 \int_{-1}^1 \pi_{t+1}(x_{t+1}, a | S_{t+1}) dx_{t+1} da}. \quad (5)$$

NUMERICAL EXPERIMENTS IN THE PERFECT MODEL SCENARIO

The *grid based method* (GBM) proceeds by constructing a uniform n_x by n_a grid of cell(i, j) where $i \in [1, n_x]$ and $j \in [1, n_a]$ on the region $[-1, 1] \times [0, 2]$. Associated with each cell is a constant value of the initial prior density, giving rise to a piecewise constant approximation to the initial prior in each cell. At time t we assume that a piecewise constant approximation is available. This is then updated at time $t+1$ at the grid points, with equation (4), using the actual values of the observations. After all the points are evaluated, the result is normalized by dividing by the integral with respect to x and a . When in predictive mode equation (2) is used.

We use the choice in [5] of $a = 1.85$, $x_0 = 0.3$ and $\sigma = 0.1$ in the numerical GBM experiments. We take uniform priors for a and for x with $x \in [-1, 1]$ and $a \in [0, 2]$. The experiment was run for 100 time steps on a 1000×1000 grid, with assimilation of observations at the end of each of the first 50 time steps. As already noted, we did not assimilate the observation of the initial state. As data was assimilated, the pdfs both before and after assimilation were analyzed. For illustrative purposes, the expectation value before assimilation was calculated, together with the 0.05 and 0.95 quantiles. After 50 time steps the experiment switched to prediction only, and data assimilation ceased.

Fig. 1 shows the observations (plotted with plus signs) and the underlying true state, without observational noise, (plotted as circles). As an estimate of the true system state, its expectation value (after assimilating the measurement) is used and plotted as crosses. The range of values of x_t , bounded by the 0.05 and 0.95 quantiles, is also plotted as gray blocks. The results are shown for the first 60 time steps. To start with, the Bayesian filter is learning the pdf for the model, here the PMS. After a few time steps the results are quite good. When assimilation is halted, at first the predictions remain good, but we see that the quantiles rapidly depart from one another, before spanning the full range of possible values for x_t . This is in accord with our intuitions regarding chaotic systems.

Fig. 2 shows evolution of the pdf $\pi_t(a | S_t)$ at intervals of 10 time steps. We remark that $\pi_t(a | S_t)$ stays unchanged when assimilation is halted, which can also be proved using equation (2). The exact value for a is 1.85. The expectation (or average) value of a after assimilation of the measurement at time step 50, is 1.859 with the 0.05 quantile at 1.848 and the 0.95 quantile at 1.888. The true value for x_0 is 0.009946. Its 0.05 quantile is at -0.029 and its 0.95 quantile is at 0.276. It therefore appears that Bayesian statistics recovers both the initial state and the parameter value quite well in the PMS, even for a high level of observational noise.

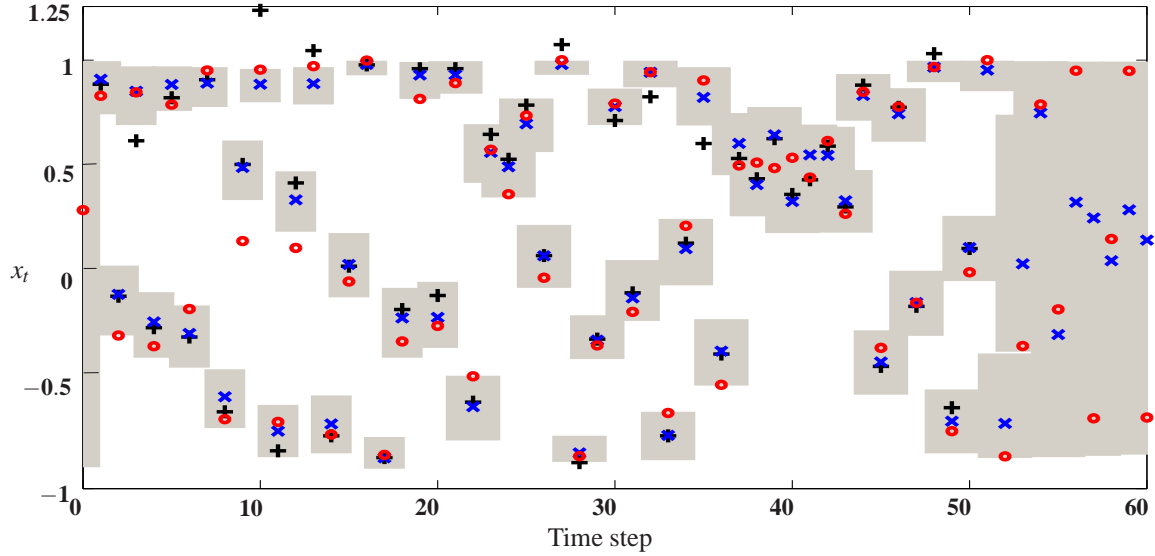


FIGURE 1. Plots of the expectation of x_t (crosses) with $\sigma=0.1$ to $t=60$, the exact states of x_t (circles), the observations s_t (pluses) in the PMS and 0.05 and 0.95 quantiles (gray).

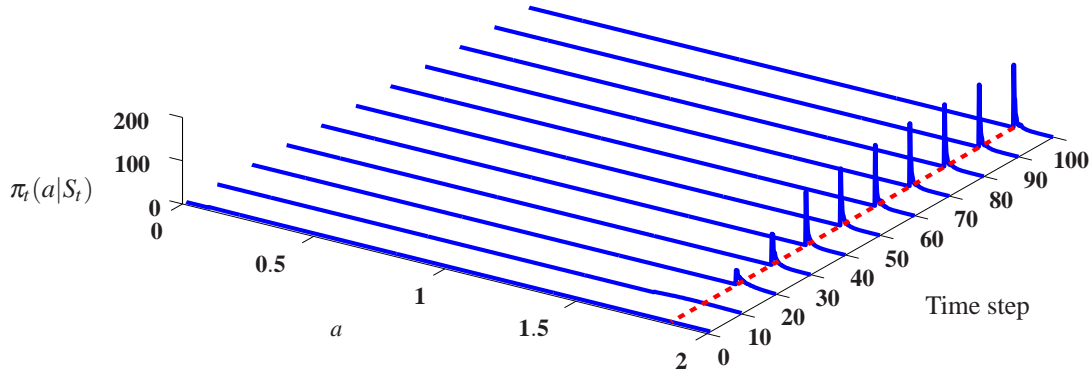


FIGURE 2. Predictive pdf for a in the high noise PMS.

DISTINGUISHING THE IMPERFECT FROM THE PERFECT MODEL SCENARIO

In the IMS, the logistic map will again be used as the postulated model. The true system is taken to be a constant state, with observations subject to noise. The true state is chosen to be a value not coinciding with an attractor of our logistic map. We take $x_n = 0.3$.

We need a test, designed to assess in which scenario we find ourselves. The suggestion proposed here is to evaluate the ‘distance’ between the predictive pdf and the pdf after assimilation at each time step during the assimilation phase. In this paper we use the Hellinger distance [6], defined by the integral:

$$h_t = \frac{1}{2} \int_{-1}^1 \int_0^2 (\sqrt{\tilde{\pi}_t} - \sqrt{\pi_t})^2 dx_t da_t.$$

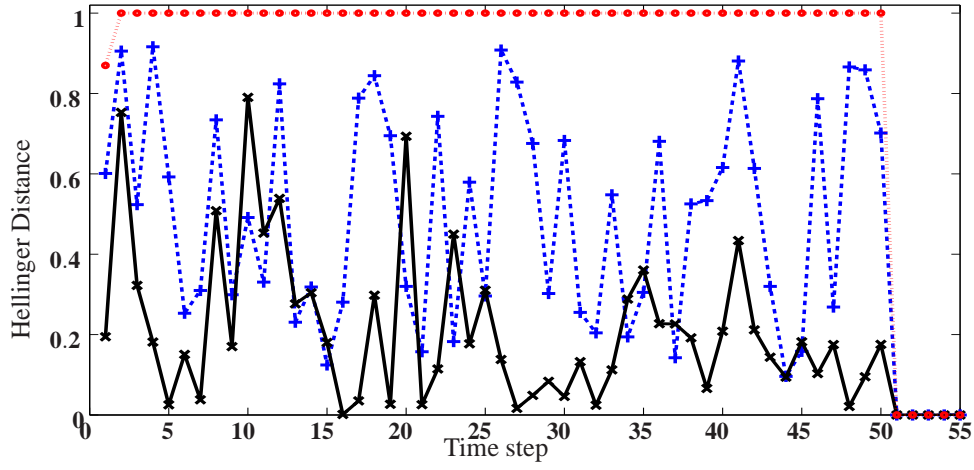


FIGURE 3. Hellinger distance distinguishing the IMS from the PMS. The high noise ($\sigma = 0.1$) PMS is shown as crosses, the high noise IMS ($\sigma = 0.1$) is shown as pluses and the low noise ($\sigma = 0.01$) IMS is shown as circles.

Fig. 3 shows h_t as a function of time for the PMS, as indicated by crosses, and the IMS with both a high ($\sigma = 0.1$) noise, as indicated by the pluses, and a low ($\sigma = 0.01$) noise (indicated by circles). The Hellinger distance is generally small for the PMS, showing that the data does not update the retrieval beyond correcting for error growth due to chaos. However, in the IMS low noise case ($\sigma = 0.01$), the Hellinger distance is nearly always close to unity; there is therefore no useful information in the data relative to the chosen model. In other words, the model (here, the logistic map) has no predictive capacity whatsoever, and so is *inadequate*. It should be noted, however, that in other applications a small Hellinger distance could be an indication of irrelevant data rather than a good or perfect model. success for the model.

DISCUSSION

In this paper we derived an exact expression for the Bayesian filter applied to the logistic map. Using numerical integration accurate estimates of both x_0 and a were possible in the PMS. By including a method of model criticism, it has been demonstrated that the analysis can indicate in which scenario - perfect or imperfect - we are located. The conclusion must be that people with good priors and good models will make better predictions than those without such knowledge. This is surely to be expected, but the unexpected conclusions are that the Bayesian approach (i) works well even in the zero-noise PMS and (ii) is, in the case studied here, able to distinguish the PMS from the IMS.

ACKNOWLEDGMENTS

This publication was based on work supported in part by Award No KUK-C1-013-04 , made by King Abdullah University of Science and Technology (KAUST).

REFERENCES

1. L. M. Berliner, *Journal of the American Statistical Association* **416**, 938–952 (1991).
2. K. Judd, and L. A. Smith, *Physica D* **151**, 125–141 (2001).
3. K. Judd, and L. A. Smith, *Physica D* **196**, 224–242 (2004).
4. C. Beck, and F. F. Schögl, *Thermodynamics of Chaotic Systems: An Introduction*, Cambridge, England: Cambridge University Press, 1993.
5. K. Judd, *Phys. Rev. E* **67** (2003).
6. D. Pollard, *A User's Guide to Measure Theoretic Probability*, Cambridge, England: Cambridge University Press, 2002.

RECENT REPORTS

12/10	Nonlinear Morphoelastic Plates I: Genesis of Residual Stress	McMahon Goriely Tabor
13/10	Nonlinear Morphoelastic Plates II: Exodus to Buckled States	McMahon Goriely Tabor
14/10	Analysis of Brownian dynamics simulations of reversible biomolecular reactions	Lipkova Zygalakis Chapman Erban
15/10	Travelling waves in hyperbolic chemotaxis equations	Xue Hwang Painter Erban
16/10	The Physics and Mechanics of Biological Systems	Goriely Moulton
17/10	Crust formation in drying colloidal suspensions	Style Peppin
18/10	A Mathematical Model of Tumor-Immune Interactions	Robertson-Tessi El-Kareh Goriely
19/10	Elastic cavitation, tube hollowing, and differential growth in plants and biological tissues	Goriely Moulton Vandiver
20/10	Asymptotic expressions for the nearest and furthest dislocations in a pile-up against a grain boundary	Hall
21/10	Cardiac electromechanics: the effect of contraction model on the mathematical problem and accuracy of the numerical scheme	Pathmanathan Chapman Gavaghan Whiteley
22/10	Fat vs. thin threading approach on GPUs: application to stochastic simulation of chemical reactions	Klingbeil Erban Giles Maini
23/10	Asymptotic analysis of a system of algebraic equations arising in dislocation theory	Hall Chapman Ockendon
25/10	Preconditioning for Allen-Cahn Variational Inequalities with Non-Local Constraints	Blank Sarbu Stoll
26/10	On an evolution equation for sand dunes	Ellis Fowler
27/10	On Liquid Films on an Inclined Plate	Benilov Chapman McLoed

29/10	A Priori Error Estimates for Semidiscrete Finite Element Approximations to Equations of Motion Arising in Oldroyd Fluids of Order One	Goswami Pani
30/10	The Landau-de Gennes theory of nematic liquid crystals: Uniaxiality versus Biaxiality	Majumdar
31/10	The Radial-Hedgehog Solution in Landau-de Gennes' theory	Majumdar
32/10	Nonlinear instability in flagellar dynamics: a novel modulation mechanism in sperm migration?	Gadelha Gaffney Smith Kirkman-Brown
33/10	Error bounds on block GaussSeidel solutions of coupled multi-physics problem	Whiteley Gillow Tavener Walter
34/10	A random projection method for sharp phase boundaries in lattice Boltzmann simulations	Reis Dellar
35/10	Regularized Particle Filter with Langevin Resampling Step	Duan Farmer Moroz

Copies of these, and any other OCCAM reports can be obtained from:

**Oxford Centre for Collaborative Applied Mathematics
Mathematical Institute
24 - 29 St Giles'
Oxford
OX1 3LB
England
www.maths.ox.ac.uk/occam**